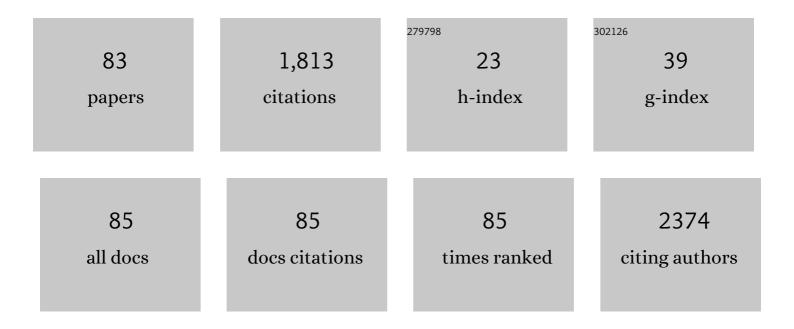
List of Publications by Year in descending order

Source: https://exaly.com/author-pdf/522565/publications.pdf Version: 2024-02-01



Ιίινο Τλε Ρλάκ

#	Article	IF	CITATIONS
1	Transition-metal-based layered double hydroxides tailored for energy conversion and storage. Journal of Materials Chemistry A, 2018, 6, 12-29.	10.3	170
2	Surface modification of silica nanoparticles with hydrophilic polymers. Journal of Industrial and Engineering Chemistry, 2010, 16, 517-522.	5.8	106
3	Preparation of TiO2 spheres with hierarchical pores via grafting polymerization and sol–gel process for dye-sensitized solar cells. Journal of Materials Chemistry, 2010, 20, 8521.	6.7	91
4	Direct Assembly of Preformed Nanoparticles and Graft Copolymer for the Fabrication of Micrometerâ€thick, Organized TiO <sub>2</sub> Films: High Efficiency Solidâ€state Dyeâ€sensitized Solar Cells. Advanced Materials, 2012, 24, 519-522.	21.0	83
5	SnO2 hollow nanotubes: a novel and efficient support matrix for enzyme immobilization. Scientific Reports, 2017, 7, 15333.	3.3	61
6	Amphiphilic poly(vinyl chloride)-g-poly(oxyethylene methacrylate) graft polymer electrolytes: Interactions, nanostructures and applications to dye-sensitized solar cells. Electrochimica Acta, 2010, 55, 4976-4981.	5.2	55
7	Facile fabrication of vertically aligned TiO2 nanorods with high density and rutile/anatase phases on transparent conducting glasses: high efficiency dye-sensitized solar cells. Journal of Materials Chemistry, 2012, 22, 6131.	6.7	55
8	High performance electrocatalyst consisting of CoS nanoparticles on an organized mesoporous SnO2 film: its use as a counter electrode for Pt-free, dye-sensitized solar cells. Nanoscale, 2015, 7, 670-678.	5.6	55
9	Excellent anti-fogging dye-sensitized solar cells based on superhydrophilic nanoparticle coatings. Nanoscale, 2014, 6, 7362-7368.	5.6	53
10	Surface-initiated atom transfer radical polymerization from TiO2 nanoparticles. Applied Surface Science, 2009, 255, 3739-3744.	6.1	52
11	Hybrid Templated Synthesis of Crackâ€Free, Organized Mesoporous TiO <sub>2</sub> Electrodes for High Efficiency Solidâ€State Dyeâ€Sensitized Solar Cells. Advanced Functional Materials, 2013, 23, 26-33.	14.9	45
12	Direct growth of highly organized, 2D ultra-thin nano-accordion Ni-MOF@NiS2@C core-shell for high performance energy storage device. Chemical Engineering Journal, 2021, 406, 126810.	12.7	45
13	Semi-interpenetrating polymer network membranes based on a self-crosslinkable comb copolymer for CO2 capture. Chemical Engineering Journal, 2019, 360, 1468-1476.	12.7	40
14	Highly Interconnected Nanorods and Nanosheets Based on a Hierarchically Layered Metal–Organic Framework for a Flexible, High-Performance Energy Storage Device. ACS Sustainable Chemistry and Engineering, 2020, 8, 3773-3785.	6.7	35
15	Improved electron transfer and plasmonic effect in dye-sensitized solar cells with bi-functional Nb-doped TiO2/Ag ternary nanostructures. Nanoscale, 2014, 6, 2718-2729.	5.6	34
16	All-solid, flexible solar textiles based on dye-sensitized solar cells with ZnO nanorod arrays on stainless steel wires. Materials Science and Engineering B: Solid-State Materials for Advanced Technology, 2013, 178, 1117-1123.	3.5	30
17	Enhancing the Performance of Solidâ€6tate Dyeâ€6ensitized Solar Cells Using a Mesoporous Interfacial Titania Layer with a Bragg Stack. Advanced Functional Materials, 2013, 23, 2193-2200.	14.9	30
18	Synthesis of amphiphilic graft copolymer brush and its use as template film for the preparation of silver nanoparticles. Journal of Polymer Science Part A, 2008, 46, 3911-3918.	2.3	27

#	Article	IF	CITATIONS
19	Templated synthesis of silver nanoparticles in amphiphilic poly(vinylidene) Tj ETQq1 1 0.784314 rgBT /Overlock 1	0 Tf 50 74 2.1	7 Td (fluoric 27
	Polymer Physics, 2008, 46, 702-709.		
20	Synthesis of hierarchical flower-shaped hollow MgO microspheres via ethylene-glycol-mediated process as a base heterogeneous catalyst for transesterification for biodiesel production. Biomass and Bioenergy, 2020, 142, 105788.	5.7	26
21	Formation of mesoporous TiO2 with large surface areas, interconnectivity and hierarchical pores for dye-sensitized solar cells. Journal of Materials Chemistry, 2011, 21, 17872.	6.7	25
22	Preparation of quasi-solid-state electrolytes using a coal fly ash derived zeolite-X and -A for dye-sensitized solar cells. Journal of Industrial and Engineering Chemistry, 2019, 71, 378-386.	5.8	25
23	Mesoporous TiO2 Bragg Stack Templated by Graft Copolymer for Dye-sensitized Solar Cells. Scientific Reports, 2014, 4, 5505.	3.3	24
24	Nanocomposite polymer electrolytes containing silica nanoparticles: Comparison between poly(ethylene glycol) and poly(ethylene oxide) dimethyl ether. Journal of Applied Polymer Science, 2007, 106, 4083-4090.	2.6	23
25	Proton conducting crosslinked membranes by polymer blending of triblock copolymer and poly(vinyl) Tj ETQq1 1	0.784314 2.4	rgBT /Overle
26	Use of block copolymer as compatibilizer in polyimide/zeolite composite membranes. Polymers for Advanced Technologies, 2011, 22, 768-772.	3.2	21
27	One-pot synthesis of hierarchical mesoporous SnO <sub>2</sub> spheres using a graft copolymer: enhanced photovoltaic and photocatalytic performance. RSC Advances, 2014, 4, 31452-31461.	3.6	21
28	Highly catalytic and reflective dual-phase nickel sulfide electrodes for solar energy conversion. Applied Surface Science, 2018, 457, 1151-1157.	6.1	21
29	Synthesis and characterization of TiO2/Ag/polymer ternary nanoparticles via surface-initiated atom transfer radical polymerization. Applied Surface Science, 2011, 257, 8301-8306.	6.1	20
30	Bragg Stackâ€Functionalized Counter Electrode for Solidâ€State Dyeâ€Sensitized Solar Cells. ChemSusChem, 2013, 6, 856-864.	6.8	19
31	Facilitated olefin transport through membranes consisting of partially polarized silver nanoparticles and PEMA-g-PPG graft copolymer. Journal of Membrane Science, 2018, 548, 149-156.	8.2	19
32	Nanocomposite membranes consisting of poly(vinyl chloride) graft copolymer and surface-modified silica nanoparticles. Macromolecular Research, 2011, 19, 1195-1201.	2.4	18
33	Multifunctional Organized Mesoporous Tin Oxide Films Templated by Graft Copolymers for Dye ensitized Solar Cells. ChemSusChem, 2014, 7, 2037-2047.	6.8	18
34	Surface Carbon Shell-Functionalized ZrO2 as Nanofiller in Polymer Gel Electrolyte-Based Dye-Sensitized Solar Cells. Nanomaterials, 2019, 9, 1418.	4.1	18
35	Composite polymer electrolyte membranes comprising P(VDFâ€ <i>co</i> â€CTFE)â€ <i>g</i> â€PSSA graft copolymer and zeolite for fuel cell applications. Polymers for Advanced Technologies, 2009, 20, 1146-1151.	3.2	17
36	Facile graft copolymer template synthesis of mesoporous polymeric metal-organic frameworks to produce mesoporous TiO2: Promising platforms for photovoltaic and photocatalytic applications. Journal of Industrial and Engineering Chemistry, 2020, 84, 384-392.	5.8	17

#	Article	IF	CITATIONS
37	Surfactant-free one-pot synthesis of Au-TiO2 core-shell nanostars by inter-cation redox reaction for photoelectrochemical water splitting. Energy Conversion and Management, 2022, 252, 115038.	9.2	16
38	Synthesis and application of PEGBEM-g-POEM graft copolymer electrolytes for dye-sensitized solar cells. Solid State Ionics, 2016, 290, 24-30.	2.7	15
39	Preparation of TiO2/Ag binary nanocomposite as high-activity visible-light-driven photocatalyst via graft polymerization. Chemical Physics Letters, 2017, 685, 119-126.	2.6	15
40	Nanofiltration membranes based on poly(vinylidene) Tj ETQq0 0 0 rgBT /Overlock 10 Tf 50 627 Td (fluorideâ€ <i> Technologies, 2008, 19, 1643-1648.</i>	co 3.2	hlorotrifluoro 14
41	Synthesis of crosslinked polystyrene-b-poly(hydroxyethyl methacrylate)-b-poly(styrene sulfonic acid) triblock copolymer for electrolyte membranes. Macromolecular Research, 2009, 17, 325-331.	2.4	14
42	Ni, Co-double hydroxide wire structures with controllable voids for electrodes of energy-storage devices. Journal of Materials Science and Technology, 2020, 55, 126-135.	10.7	14
43	1D Co4S3 nanoneedle array with mesoporous carbon derived from double comb copolymer as an efficient solar conversion catalyst. Applied Surface Science, 2021, 535, 147637.	6.1	14
44	Graft polymerization of poly(epichlorohydrin-g-poly((oxyethylene) methacrylate)) using ATRP and its polymer electrolyte with KI. Ionics, 2009, 15, 163-167.	2.4	13
45	Structural color-tunable mesoporous bragg stack layers based on graft copolymer self-assembly for high-efficiency solid-state dye-sensitized solar cells. Journal of Power Sources, 2016, 324, 637-645.	7.8	13
46	Solid-State Solar Energy Conversion from WO3 Nano and Microstructures with Charge Transportation and Light-Scattering Characteristics. Nanomaterials, 2019, 9, 1797.	4.1	13
47	Synthesis of Ag <sub>2</sub> O decorated hierarchical TiO <sub>2</sub> templated by double comb copolymers for efficient solar water splitting. Chemical Communications, 2019, 55, 11013-11016.	4.1	12
48	Imidazole-functionalized hydrophilic rubbery comb copolymers: Microphase-separation and good gas separation properties. Separation and Purification Technology, 2020, 242, 116780.	7.9	12
49	Formation of silver nanoparticles created <i>in situ</i> in an amphiphilic block copolymer film. Journal of Applied Polymer Science, 2008, 110, 2352-2357.	2.6	11
50	Mixed matrix membranes consisting of ZIF-8 in rubbery amphiphilic copolymer: Simultaneous improvement in permeability and selectivity. Chemical Engineering Research and Design, 2020, 153, 175-186.	5.6	11
51	Harnessing SnO2 nanotube light scattering cluster to improve energy conversion efficiency assisted by high reflectance. Materials Chemistry and Physics, 2020, 254, 123538.	4.0	11
52	Ultrathin, Highly Permeable Graphene Oxide/Zeolitic Imidazole Framework Polymeric Mixed-Matrix Composite Membranes: Engineering the CO <sub>2</sub> -Philic Pathway. ACS Sustainable Chemistry and Engineering, 2021, 9, 11903-11915.	6.7	11
53	A highly efficient nanofibrous air filter membrane fabricated using electrospun amphiphilic PVDF-g-POEM double comb copolymer. Separation and Purification Technology, 2021, 279, 119625.	7.9	11
54	Multifunctional all-TiO <sub>2</sub> Bragg stacks based on blocking layer-assisted spin coating. Journal of Materials Chemistry C, 2014, 2, 3260-3269.	5.5	10

#	Article	IF	CITATIONS
55	Surface-controlled galvanic replacement for the development of Pt-Ag nanoplates with concave surface substructures. Chemical Engineering Journal, 2021, 417, 128026.	12.7	10
56	Proton-conducting composite membranes from graft copolymer electrolytes and phosphotungstic acid for fuel cells. Ionics, 2009, 15, 439-444.	2.4	9
57	Molecular thermodynamic model of the glass transition temperature: dependence on molecular weight. Polymers for Advanced Technologies, 2008, 19, 944-946.	3.2	8
58	Synthesis of organized mesoporous metal oxide films templated by amphiphilic PVA–PMMA comb copolymer. RSC Advances, 2016, 6, 67849-67857.	3.6	8
59	Environmental friendly synthesis of hierarchical mesoporous platinum nanoparticles templated by fucoidan biopolymer for enhanced hydrogen evolution reaction. Journal of Materials Science and Technology, 2020, 46, 185-190.	10.7	8
60	Reliability-Based Robust Design Optimization of Lithium-Ion Battery Cells for Maximizing the Energy Density by Increasing Reliability and Robustness. Energies, 2021, 14, 6236.	3.1	8
61	Shape-Controlled TiO2 Nanomaterials-Based Hybrid Solid-State Electrolytes for Solar Energy Conversion with a Mesoporous Carbon Electrocatalyst. Nanomaterials, 2021, 11, 913.	4.1	7
62	Templated formation of silver nanoparticles using amphiphilic poly(epichlorohydrine-g-styrene) film. Macromolecular Research, 2009, 17, 301-306.	2.4	6
63	Sensitive and Homogeneous Surfaceâ€Enhanced Raman Scattering Detection Using Heterometallic Interfaces on Metal–Organic Frameworkâ€Derived Structure. Advanced Materials Interfaces, 2022, 9, .	3.7	6
64	Ultrafiltration membranes based on hybrids of an amphiphilic graft copolymer and titanium isopropoxide. Journal of Applied Polymer Science, 2018, 135, 45932.	2.6	5
65	Synthesis, structure and gas separation properties of ethanol-soluble, amphiphilic POM-PBHP comb copolymers. Polymer, 2019, 180, 121700.	3.8	5
66	Impregnation approach for poly(vinylidene fluoride)/tin oxide nanotube composites with high tribological performance. Journal of Materials Science and Technology, 2020, 37, 19-25.	10.7	5
67	High-order diffraction grating as light harvesters for solar energy conversion. Journal of Electroanalytical Chemistry, 2020, 873, 114490.	3.8	5
68	High-voltage solar energy conversion based on ZIF-67-derived binary redox-quasi-solid-state electrolyte. Journal of Electroanalytical Chemistry, 2021, 893, 115264.	3.8	5
69	Synthesis of binary metal–metal oxide coreâ€shell nanoparticles via surfactantâ€free intercation redox reactions. Bulletin of the Korean Chemical Society, 2022, 43, 1002-1006.	1.9	5
70	Well-organized mesoporous TiO2 film with high porosity made using alcohol-assisted EC-g-PMMA graft copolymer. Macromolecular Research, 2016, 24, 573-576.	2.4	4
71	Fogging, reflection, and dust-free transparent conducting glasses based on superhydrophilic nanotextures for organic photovoltaics. Journal of Industrial and Engineering Chemistry, 2017, 52, 243-250.	5.8	4
72	One-dimensional SnO2 nanotube solid-state electrolyte for fast electron transport and high light harvesting in solar energy conversion. Solid State Ionics, 2021, 363, 115584.	2.7	4

#	Article	IF	CITATIONS
73	Preparation of Co9S8 nanostructure with double comb copolymer derived mesoporous carbon for solar energy conversion catalyst. Journal of Electroanalytical Chemistry, 2021, 895, 115384.	3.8	4
74	Polymer Electrolytes Based on Grafted Inorganic Nanoparticles for Dye-Sensitized Solar Cells. Journal of Nanoscience and Nanotechnology, 2011, 11, 1718-1721.	0.9	3
75	Designing double comb copolymer as highly lithium ionic conductive solid-state electrolyte membranes. Reactive and Functional Polymers, 2021, 169, 105093.	4.1	3
76	One-step Fabrication of Crack-free, Hierarchically-ordered TiO2 Films via Self-assembly of Polystyrene Bead and Preformed TiO2. Electrochimica Acta, 2014, 117, 521-527.	5.2	2
77	Tailored ZnO Nanostructure Based Quasi-Solid-State Electrolyte and Mesoporous Carbon Electrocatalyst for Solar Energy Conversion. ECS Journal of Solid State Science and Technology, 2021, 10, 085005.	1.8	2
78	Prediction of the glass transition temperature of semicrystalline polymer/salt complexes. Journal of Polymer Science, Part B: Polymer Physics, 2009, 47, 793-798.	2.1	1
79	Quasi-Solid-State SiO2 Electrolyte Prepared from Raw Fly Ash for Enhanced Solar Energy Conversion. Materials, 2022, 15, 3576.	2.9	1
80	Hierarchical TiO <inf>2</inf> spheres architectures for quasi solid state dye-sensitized solar cells by living radical polymerization and sol-gel process. , 2011, , .		0
81	Nanostructural TiO <inf>2</inf> films with high surface areas and controllable pore sizes for high performance dye-sensitized solar cells. , 2011, , .		Ο
82	Multifunctional Organized Mesoporous Tin Oxide Films Templated by Graft Copolymers for Dye-Sensitized Solar Cells. ChemSusChem, 2014, 7, 1767-1767.	6.8	0
83	Sensitive and Homogeneous Surfaceâ€Enhanced Raman Scattering Detection Using Heterometallic Interfaces on Metal–Organic Frameworkâ€Derived Structure (Adv. Mater. Interfaces 7/2022). Advanced Materials Interfaces, 2022, 9, .	3.7	0